Artesunate Derived from Traditional Chinese Medicine Induces DNA Damage and Repair

Paul C.H. Li,[1] Elena Lam,[1] Wynand P. Roos,[1] Małgorzata Z. Zdzienicka,[3] Bernd Kaina,[1] and Thomas Efferth[2]

[1]Institute of Toxicology, University of Mainz, Mainz, Germany; [2]Pharmaceutical Biology (C015), German Cancer Research Center, Heidelberg, Germany; and [3]Department of Molecular Cell Genetics, UMK Collegium Medicum, Bydgoszcz, Poland

Abstract

Artesunate is a semisynthetic derivative from artemisinin, a natural product from the Chinese herb *Artemisia annua* L. It exerts antimalarial activity, and, additionally, artemisinin and its derivatives are active against cancer cells. The active moiety is an endoperoxide bridge. Its cleavage leads to the formation of reactive oxygen species and carbon-centered radicals. These highly reactive molecules target several proteins in *Plasmodia*, which is thought to result in killing of the microorganism. DNA damage induced by artemisinins has not yet been described. Here, we show that artesunate induces apoptosis and necrosis. It also induces DNA breakage in a dose-dependent manner as shown by single-cell gel electrophoresis. This genotoxic effect was confirmed by measuring the level of γ-H2AX, which is considered to be an indication of DNA double-strand breaks (DSB). Polymerase β–deficient cells were more sensitive than the wild-type to artesunate, indicating that the drug induces DNA damage that is repaired by base excision repair. irs1 and VC8 cells defective in homologous recombination (HR) due to inactivation of XRCC2 and BRCA2, respectively, were more sensitive to artesunate than the corresponding wild-type. This was also true for XR-V15B cells defective in nonhomologous end-joining (NHEJ) due to inactivation of Ku80. The data indicate that DSBs induced by artesunate are repaired by the HR and NHEJ pathways. They suggest that DNA damage induced by artesunate contributes to its therapeutic effect against cancer cells. [Cancer Res 2008;68(11):4347–51]

Introduction

Artemisinin is a sesquiterpene isolated from *Artemisia annua* L., which is used in traditional Chinese medicine for the treatment of fever and chills (1). Artemisinin has profound activity against *Plasmodium falciparum* and *Plasmodium vivax* (2). Artesunate and artemether are semisynthetic derivatives of artemisinin. In addition to their antimalarial activity, artemisinin and its derivatives are also active against cancer cells (3–7).

The active moiety of artemisinins is an endoperoxide bridge. In *Plasmodia*, the cleavage of the endoperoxide moiety is facilitated by heme iron released during hemoglobin digestion of *Plasmodia* in erythrocytes of the host. In a Fe(II) Fenton reaction, reactive oxygen species, such as hydroxyl radicals and superoxide anions, are generated (8). Furthermore, carbon-centered radical species are generated by decomposition of artemisinins (9). These highly reactive molecules alkylate heme and several other proteins, such as translationally controlled tumor protein, histidine-rich protein (42 kDa), and pfATP6, the sarco/endoplasmatic reticulum calcium ATPase (10, 11). Recent observations indicate that oxidative stress also plays a role in the activity of artemisinins against cancer cells (12, 13). Whereas protein alkylation by artemisinin and its derivatives has been well established, damage of DNA has not yet been reported in *Plasmodia* (14).

In this study, we have readdressed the question of whether artesunate induces DNA damage. The rationale for this study was the findings that (*a*) concentrations required for inhibiting cancer cells are about 1 to 2 orders of magnitude higher than those for killing *Plasmodia* and (*b*) radicals derived from artesunate are expected to attack various types of molecules, including DNA. To prove this, we first measured DNA damage by the comet assay and γ-H2AX phosphorylation. To see which mode of DNA repair is important for artesunate-induced DNA damage, we then investigated cell lines with defined molecular defects in the main DNA repair pathways [e.g., nucleotide excision repair (NER), base excision repair (BER), nonhomologous end-joining (NHEJ), homologous recombination (HR), and damage reversal by O^6-methylguanine DNA methyltransferase (MGMT)].

Materials and Methods

Materials and cell lines. Antibodies used for Western blotting were purchased from Santa Cruz Biotechnology, Inc. and Upstate. For the experiments, we used the following cell lines. (*a*) Chinese hamster ovary cell line CHO-9 and the NER-deficient derivatives 27-1 and 43-3B (15). The 27-1 cells are mutated in ERCC3, whereas 43-3B cells are mutated in ERCC1. The cells were cultured in DMEM/F12 containing Glutamax (Life Technologies) and 5% heat-inactivated FCS. (*b*) The parental hamster lung fibroblast cell line V79-2 and their HR-deficient derivatives VC8, VC8 MGMT, and VC8 mouse bacterial artificial chromosome (mBAC). The VC8 cells are defective in the *BRCA2* gene. VC8 MGMT cells are transfected with the *MGMT* gene and express MGMT at high level (data not shown). VC8 mBAC was generated by chromosomal complementation of VC8. (*c*) The parental Chinese hamster lung fibroblast cell line V79wt and its HR-deficient derivative irs1. The irs1 cells are defective in the *XRCC2* gene (supplied by Dr. Margaret Zdienicka). (*d*) The parental Chinese hamster lung fibroblast cell line V79-B and the NHEJ-deficient derivative XR-V15B, which is defective in the *Ku80* gene. These cell lines were cultured in RPMI 1640 and 10% heat-inactivated FCS. (*e*) The parental mouse fibroblast cell line polymerase $\beta^{+/+}$ (Pol$\beta^{+/+}$) and the BER-defective derivative Pol$\beta^{-/-}$, which is defective in Polβ (kindly provided by R. Sobol, Hillman Cancer Center, Pittsburgh, PA; ref. 16). These cell lines were cultured in DMEM/high-glucose medium and 10% heat-inactivated FCS.

Artesunate treatment. For the survival assays, the cells were treated with artesunate continuously after 6 h of seeding. For Western blot

Note: P.C.H. Li and E. Lam contributed equally to this work.

Current address for P.C.H. Li: Department of Chemistry, Simon Fraser University, Burnaby, British Columbia, Canada.

Requests for reprints: Thomas Efferth, Pharmaceutical Biology (C015), German Cancer Research Center, Im Neuenheimer Feld 280, 69120 Heidelberg, Germany. Phone: 49-6221-423426; E-mail: t.efferth@dkfz.de.

doi:10.1158/0008-5472.CAN-07-2970

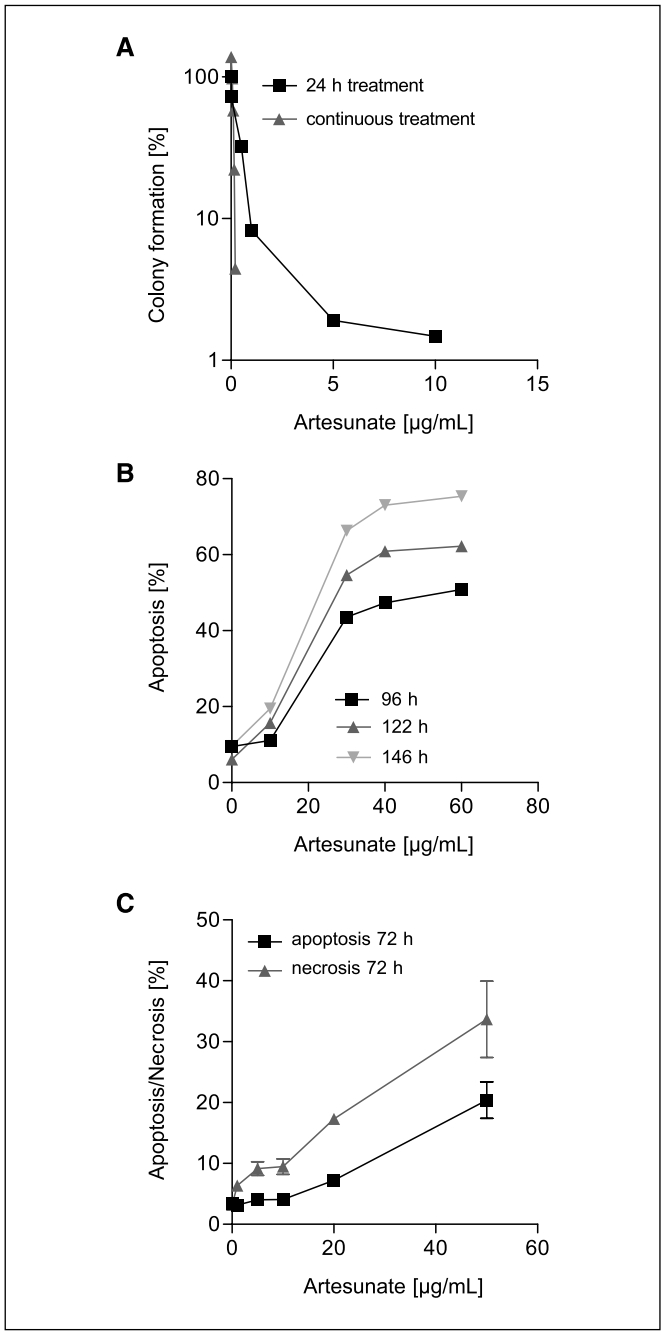

Figure 1. Cell death induced by artesunate. *A,* CHO-9 cells were treated with artesunate continuously or for 24 h and colony formation was determined 7 d later. *B,* induction of apoptosis in CHO-9 cells as a function of dose of artesunate (continuous treatment) as measured 96, 122, and 146 h after treatment by sub-G_1 analysis. *C,* induction of apoptosis and necrosis by artesunate as a function of dose, as measured 72 h after treatment by Annexin V/propidium iodide flow cytometry.

experiments, apoptosis/necrosis measurement, and the γ-H2AX foci staining, the cells were treated after 24 h of seeding continuously with artesunate.

Clonogenic survival experiments. Cells (up to 500 per plate) were seeded into 6-cm dishes. After 6 h, they were treated with concentrations of artesunate ranging between 1 and 5 μg/mL (if not otherwise stated continuously). Artesunate was dissolved in DMSO and then diluted (1:1) in H_2O to a final stock solution of 2 mg/mL. One week later, colonies were fixed with methanol and stained with 1.25% Giemsa and 0.125% crystal violet for counting. Cell survival was expressed in relation to the untreated control. Values are given as mean of three independent experiments.

Single-cell gel electrophoresis (comet assay). Single-strand breaks were determined and quantified by the highly sensitive neutral single-cell gel electrophoresis assay (comet assay) as previously described (17). In brief, cells were embedded in 0.5% low melting point agarose, and microscope slides were immersed in ice-cold lysis solution [2.5 mol/L NaCl, 100 mmol/L EDTA, 10 mmol/L Tris, 1% sodium laurylsarcosine (pH 7), 1% Triton X-100, and 10% DMSO were added freshly] and maintained at 4°C for 1 h. After lysis, electrophoresis (25 V) was performed at 4°C for 15 min in 90 mmol/L Tris, 90 mmol/L boric acid, and 2 mmol/L EDTA (pH 7.5). The fixed and ethidium bromide–stained slides were analyzed using a fluorescence microscope. The analysis of DNA migration was performed by an image analysis system (Kinetic Imaging Ltd.; Komet 4.0.2; Optilas), determining the median tail moment (percentage of DNA in the tail/tail length) of 50 cells per sample.

Quantification of apoptosis. For determination of apoptotic and necrotic cells, flow cytometric analysis with Annexin V/FITC–stained and propidium iodide–stained cells was performed as described. Cells were trypsinized, washed in PBS, and resuspended in 30 μL cold Annexin V binding buffer [10 mmol/L HEPES (pH 7.4), 0.14 mol/L NaCl, 0.25 mmol/L $CaCl_2 \cdot 2\ H_2O$, 0.1% bovine serum albumin (BSA; w/v)]. After addition of 1.5 μL Annexin/FITC (Becton Dickinson), cells were incubated in the dark for 15 to 30 min. At least 264 μL binding buffer and 6 μL propidium iodide (50 μg/mL) were added per sample. Samples were analyzed using a FACSort flow cytometer (Becton Dickinson). Values are given as mean of three independent experiments.

For determination of apoptotic cells, cells were trypsinized, washed in PBS, and resuspended in 100 μL cold PBS. Afterwards, 2 mL of ice-cold 70% ethanol were added per sample and the samples were kept at −20°C for at least 15 min and up to 5 d. Following centrifugation, cells were resuspended in 333 μL PBS containing RNase (0.03 μg/mL) and incubated for 1 h at room temperature in the dark. Afterwards, 164 μL propidium iodide (50 μg/mL) was added to the samples. Samples were analyzed using a FACSort flow cytometer. Values are given as mean of three independent experiments.

Preparation of protein extracts. Cells were harvested by trypsinization, washed twice with PBS, and resuspended in whole-cell extract buffer [1 mmol/L EDTA, 20 mmol/L Tris, 1 mmol/L β-mercaptoethanol, 5% glycine (pH 8.5), 1 mmol/L DTT, 0.5 mmol/L phenylmethylsulfonyl fluoride]. Then, cells were disrupted (2 × 10 pulse, 40 duty cycles) on ice using the Branson Sonifier Cell Disruptor B15. To remove cell debris, the suspension was centrifuged (10,000 × *g* for 15 min). The supernatants were collected and the protein concentration was determined.

Western blot analysis. Protein (30 μg per sample) was separated in a 10% to 15% SDS-polyacrylamide gel by electrophoresis. Thereafter, proteins were blotted onto a nitrocellulose membrane (Protran, Schleicher and Schuell) overnight. Membranes were blocked for 1 h in 5% (w/v) milk powder in TBS [10× TBS: 24.2 g Tris, 80 g NaCl (pH 7.6), in 1 L H_2O] containing 0.1% Tween 20 (T-TBS), incubated overnight with the primary antibody (1:1,000–1:3,000 dilution), washed thrice for 10 min with T-TBS, and incubated for 2 h with anti-mouse, anti-rabbit secondary antibody (1:4,000). After the final washing with T-TBS (10 min for three times), blots were developed by using a chemiluminescence detection system (Amersham).

γ-H2AX immunofluorescence staining. Coverslips were cleaned for 10 min with diethylether and washed with 100% ethanol, 70% ethanol, and H_2O_{dest} for 20 min in 1 mol/L HCl; afterwards, the coverslips were kept in 70% ethanol. Cells (10^5) were seeded on clean coverslips in a 6-cm dish. The cells were treated 24 h after seeding with different doses of artesunate. Twenty-four hours after treatment, the cells on the coverslips were washed with PBS and fixed with 4% paraformaldehyde in PBS for 15 min. After cross-linking, the cells on the coverslips were washed thrice for 5 min with PBS. Ice-cold methanol (100%) was added to the paraformaldehyde cross-linked cells on the coverslips and kept at −20°C for 20 min. Thereafter, the coverslips were blocked with 5% BSA in PBS and 0.3% Triton X-100 for 1 h.

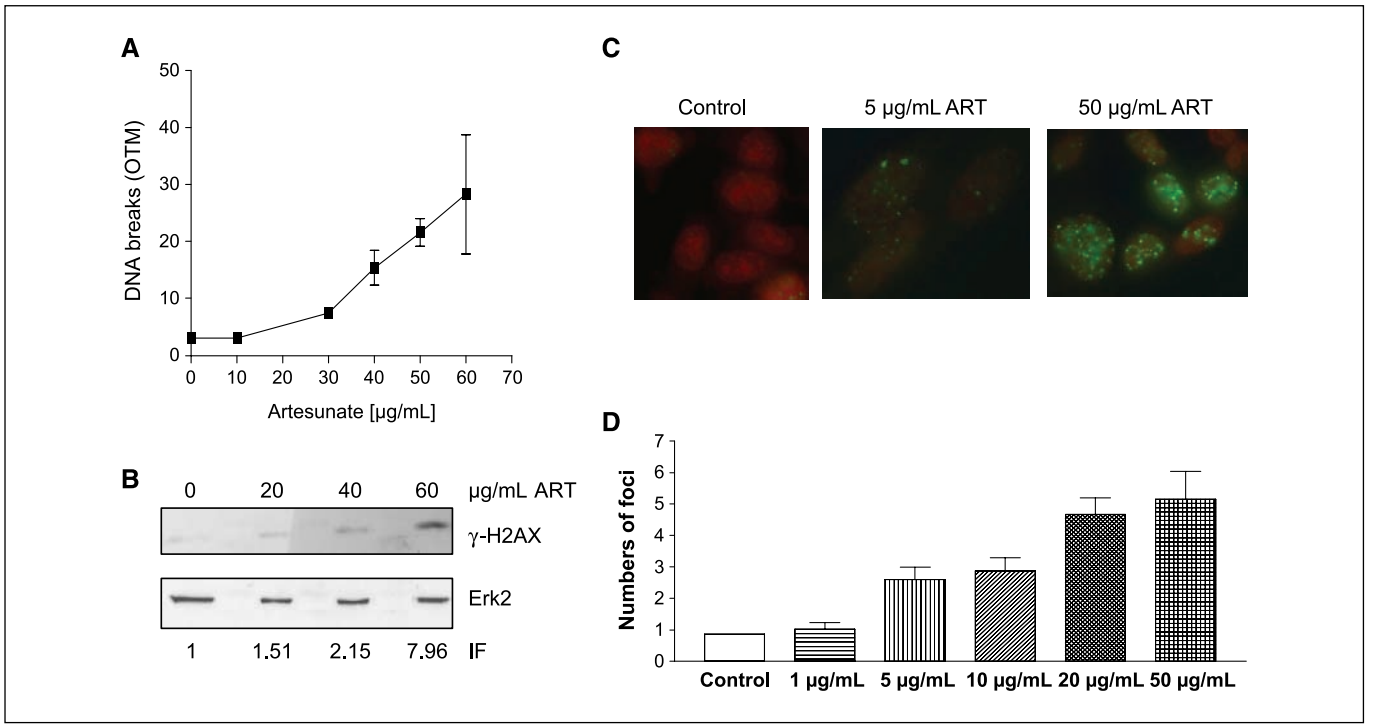

Figure 2. Induction of DNA strand breaks by artesunate. *A,* exponentially growing CHO-9 cells were exposed to artesunate for 24 h, harvested, and subjected to alkaline single-cell gel electrophoresis. *Points,* mean of three independent experiments; *bars,* SD. *B,* CHO-9 cells were exposed to artesunate (*ART*) for 24 h, harvested, and subjected to Western blot analysis. As loading control, the filter was reincubated with extracellular signal-regulated kinase 2 (*Erk2*). Induction factors (*IF*) were calculated by densitometric measurements of γ-H2AX and related to Erk2. *C,* immunohistochemical staining of cells not treated (*Control*) and treated with artesunate for 24 h. Nuclei were stained red with propidium iodide; γ-H2AX foci are the green fluorescent dots on the red background. *D,* quantification of γ-H2AX foci in CHO-9 cells treated for 24 h with artesunate.

The blocking medium was removed and 50 μL of primary antibody γ-H2AX (1:1,000 in PBS + 0.3% Triton X-100) were added directly onto the coverslips and kept at 4°C overnight. The next day, the coverslips were washed twice for 5 min with PBS and once for 2 min with high-salt PBS (PBS + 0.4 mol/L NaCl). Afterwards, 50 μL of the secondary antibody (anti-γ-H2AX Alexa Fluor 488, 1:500 in PBS + 0.3% Triton X-100) were added onto the coverslips and incubated for 1 h at room temperature in the dark. Then, the coverslips were again washed (in the dark) twice for 5 min with PBS and once with high-salt PBS. Antifade medium [10 μL; glycerol/PBS (1:1), 2.5% DABCO (pH 8.6), 1 μmol/L propidium iodide, 100 μg/mL RNase] was added on slides and the coverslips were put on the slides. Then, the coverslips were sealed with nail varnish to prevent drying and kept in the dark at 4°C. The slides were analyzed with a fluorescence microscope.

Results

First, we studied the effect of artesunate on cell survival. As shown in Fig. 1*A*, artesunate is clearly more cytotoxic if treatment occurs permanently compared with 24 h. Measurement of apoptosis by sub-G_1 flow cytometry revealed that artesunate induces apoptosis dose and time dependently (Fig. 1*B*). It was also able to induce necrosis, which is even higher than the level of

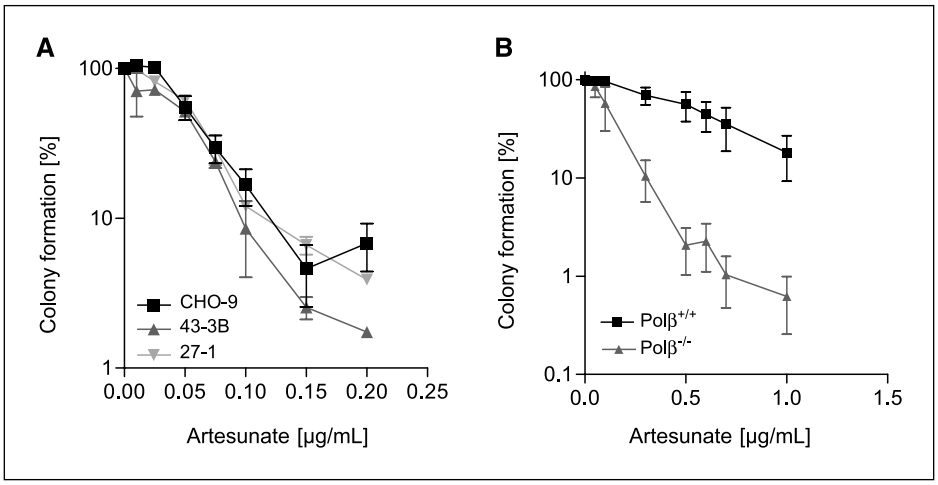

Figure 3. Cytotoxicity of artesunate in NER- and BER- defective cells. *A,* cytotoxic effect of artesunate in CHO-9 cells and their NER-defective derivatives 43-3B and 27-1 and (*B*) in mouse wild-type fibroblasts (Polβ$^{+/+}$) and the corresponding BER-defective cells (Polβ$^{-/-}$). Cytotoxicity was determined by means of colony formation. *Points,* mean of three independent experiments; *bars,* SD.

apoptosis, as determined by Annexin V/propidium iodide flow cytometry (Fig. 1*C*).

The genotoxic potential of artesunate was determined by alkaline single-cell gel electrophoresis. As shown in Fig. 2, the drug induces significant DNA breakage that increases with dose. This genotoxic effect was verified by measuring the level of γ-H2AX, which is considered to be related to DNA double-strand break (DSB) formation. The overall γ-H2AX level increased in the same dose range in which cells responded in the comet assay (Fig. 3*A*). This was confirmed by immunohistochemistry on cellular level, which revealed that already after treatment with 5 μg/mL artesunate significant γ-H2AX foci were induced (Fig. 3*B*). The data show that artesunate is able to induce DNA damage that either represent DSBs or will be converted into DSBs.

If artesunate is able to induce DNA damage, it is anticipated that DNA repair-defective cells are more sensitive than the corresponding wild-type cells to artesunate. To prove this hypothesis, we determined the cytotoxic response of different well-described repair-deficient cell lines toward artesunate. As shown in Fig. 3*A*, 43-3B and 27-1 cells defective in NER are not clearly more sensitive to artesunate, indicating that the drug does not induce bulky DNA lesions. Interestingly, Polβ-deficient cells were highly sensitive to artesunate (Fig. 3*B*). Polβ is a key enzyme in BER, indicating that artesunate-induced DNA damage is repaired by the BER pathway.

DNA base damage can be converted into DSBs that are repaired by NHEJ and HR. Therefore, we studied the effect of artesunate on mutants defective in the repair of DSBs. irs1 cells defective in HR were more sensitive to artesunate than the wild-type (Fig. 4*A*). Even more dramatic was the response of VC8 cells (Fig. 4*B*), defective in HR due to mutational inactivation of BRCA2. Complementation of VC8 cells generating the clone VC8 mBAC (18) partially rescued the artesunate hypersensitive phenotype (Fig. 4*B*), which is to be expected if the hypersensitivity to artesunate is due to the HR repair defect. Transfection with MGMT did not result in significant increase in survival of VC8 cells, indicating that DNA methylation damage is very likely not involved in artesunate-induced cell death. Similar to the previous lines, V15B cells defective in Ku80 were also more sensitive to artesunate. Ku80 is involved in NHEJ, indicating that this DSB repair pathway may also play a role in repairing artesunate-induced DNA damage.

Discussion

In this investigation, we show that artesunate is able to induce DNA damage and apoptosis. DNA damage was quantified by the alkaline comet assay that determines DNA single-strand breaks. We further found that cells defective in NER were not more sensitive to artesunate, which suggests that artesunate does not induce bulky DNA lesions that are subject to repair by NER. However, cells defective in Polβ, which is a key enzyme in BER (16), were clearly more sensitive than the corresponding wild-type to artesunate. This implies that artesunate causes DNA damage that is repaired by BER. Given the role of artesunate in the oxidative stress response in *Plasmodia*, it is pertinent to conclude that artesunate induces oxidative DNA damage in mammalian cells, which directly or indirectly (i.e., replication mediated) results in the formation of DNA breaks.

We further showed that artesunate induces the formation of DSBs, as determined by γ-H2AX phosphorylation, which occurred 24 to 48 h after treatment with a dose of >5 μg/mL and proceeded cell death by apoptosis. If DSBs are induced, it would be expected that cells defective in DSB repair are more sensitive to artesunate. This was indeed the case. Cells displaying a defect in the HR pathway due to mutational inactivation of XRCC2 or BRCA2 proved to be hypersensitive toward artesunate. Cells exhibiting a defect in NHEJ due to inactivation of Ku80 were also more sensitive. This suggests that both HR and NHEJ play a role in the repair of DSBs that arose from exposure to artesunate. Because HR is the major pathway of DSB repair in the S phase, it is

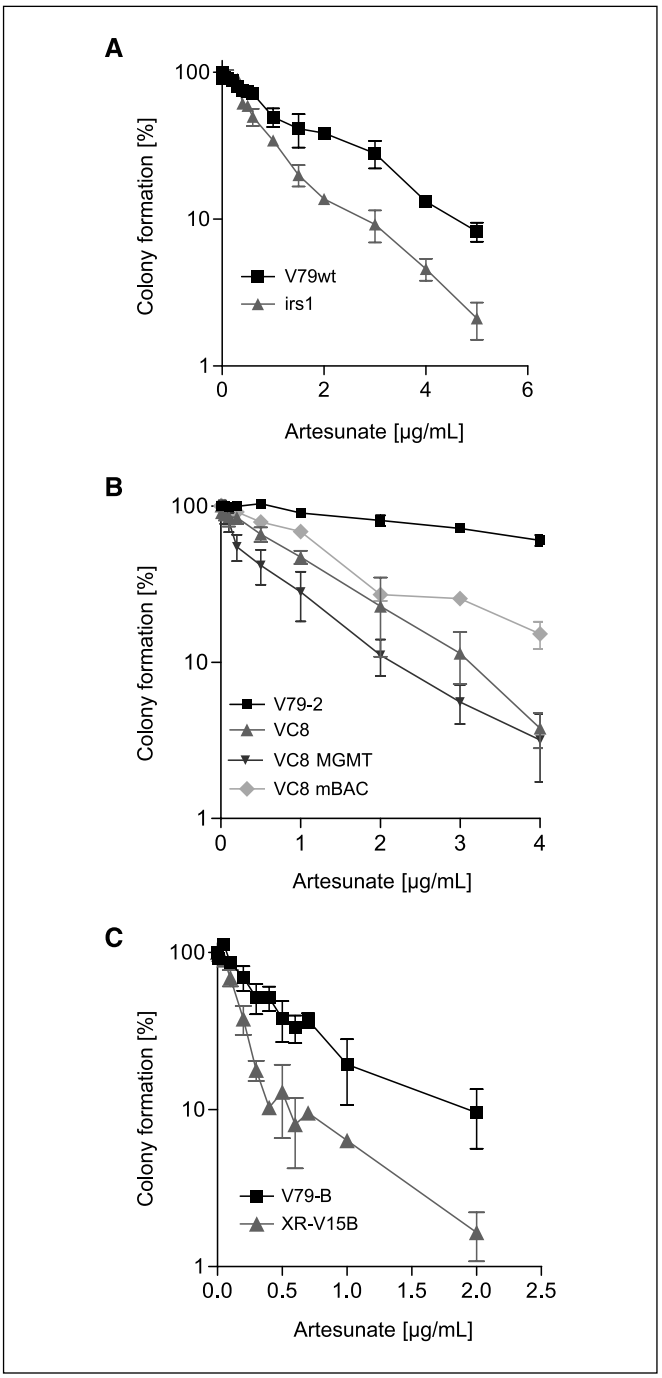

Figure 4. Cytotoxicity of artesunate in DSB repair-defective cells. Cell killing measured by colony formation was induced in V79wt and irs1 cells defective in XRCC2 (*A*); V79-2 cells and VC8 defective in BRCA2, as well as VC8 MGMT (VC8 transfected with MGMT) and VC8 mBAC (VC8 stably complemented by BAC-mediated gene transfer; *B*); and V79-B and XR-V15B cells defective in Ku80 (*C*). *Points,* mean of tree independent experiments; *bars,* SD.

pertinent to conclude that at least a part of the DSBs observed arose from interference of artesunate-induced DNA lesions with the DNA replication machinery.

Overall, the data support the role of oxidative DNA damage and DSBs as the underlying reason for the anticancer effect of artesunate, which is mediated by the induction of apoptosis. We should note that, in the course of investigations on the use of artemisinin and artesunate to treat malaria, artemisinin has been found to bind to certain target proteins, but not to DNA (14). This may be due to the fact that artemisinin and its derivatives are active toward *Plasmodia* at much lower concentrations than the concentrations required for causing DNA damage. It may also indicate that DNA damage is not caused by direct binding of artesunate to DNA but because of induction of oxidative stress. This may occur at higher dose level in mammalian cells than in *Plasmodia*, which may explain the low systemic side effects in malaria therapy.

Similarly, the tumor specificity of artesunate might be explained based on high-level induction of oxidative DNA damage in tumor cells compared with normal cells. Alternatively, it is pertinent to speculate that tumor cells are less efficient in repairing artesunate-induced DNA damages, notably DSBs, and/or execute better apoptosis. Nevertheless, is has to be considered that the genotoxicity of artesunate may lead to adverse side effects in some normal tissues. Although artesunate does not reveal severe side effects during malaria therapy (19), experiments in animals revealed neurotoxicity at supratherapeutic doses (20). As higher concentrations of artesunate are required to kill cancer cells, compared with the treatment of malaria, it has to be taken into account that artesunate might be neurotoxic in cancer treatment. In line with this view are data showing that artemisinin produces reactive oxygen species that inhibit brain stem cell cultures (21). The authors found that mRNA expression levels of manganese-dependent superoxide dismutase decreased on artemisinin treatment due to mitochondrial dysfunction. In our analyses, we treated cells transfected with cDNAs for heavy and light chains of γ-glutamylcysteine synthetase (γ-GCS) with artesunate. Because γ-GCS is the rate-limiting enzyme in the biosynthesis of the detoxifying molecule glutathione, it is expected that transfected cells are resistant to artesunate. Indeed, we found a 2.5-fold increase of resistance of transfected cells compared with mock controls (22). Moreover, we used L-buthionine sulfoximine (BSO), which is a specific inhibitor of glutathione, thus depleting glutathione pools. BSO sensitized γ-GCS–transfected cells for artesunate to a level comparable with mock vector–transfected cells (22). BSO also increased neurotoxic effects of nontoxic concentrations of other artemisinin derivatives, artemether and dihydroartemisinin, suggesting that endogenous glutathione participates in the prevention of neurotoxicity of artemisinins (23). All of these findings are consistent with a role of artesunate in mediating DNA damage by oxidative stress.

Acknowledgments

Received 8/2/2007; revised 11/16/2007; accepted 3/7/2008.

Grant support: DFG-Ka724/13-3, Stiftung Rheinland Pfalz, and Royal Society of Chemistry travel grant (P.C.H. Li).

The costs of publication of this article were defrayed in part by the payment of page charges. This article must therefore be hereby marked *advertisement* in accordance with 18 U.S.C. Section 1734 solely to indicate this fact.

References

1. Klayman DL. Qinghaosu (artemisinin): an antimalarial drug from China. Science 1985;228:1049–55.
2. Efferth T. Willmar Schwabe Award 2006: antiplasmodial and antitumor activity of artemisinin—from bench to bedside. Planta Med 2007;73:299–309.
3. Woerdenbag HJ, Moskal TA, Pras N, et al. Cytotoxicity of artemisinin-related endoperoxides to Ehrlich ascites tumor cells. J Nat Prod 1993;56:849–56.
4. Efferth T, Rücker G, Falkenberg M et al. Detection of apoptosis in KG-1a leukemic cells treated with investigational drugs. Arzneimittelforschung 1996;46:196–200.
5. Efferth T, Dunstan H, Sauerbreys A, Miyachi H, Chitambar CR. The antimalarial artesunate is also active against cancer. Int J Oncol 2001;18:767–73.
6. Efferth T, Sauerbrey A, Olbrich A, et al. Molecular modes of action of artesunate in tumor cell lines. Mol Pharmacol 2003;64:382–94.
7. Singh NP, Lai H. Selective toxicity of dihydroartemisinin and holotransferrin toward human breast cancer cells. Life Sci 2001;70:49–56.
8. Berman PA, Adams PA. Artemisinin enhances heme-catalyzed oxidation of lipid membranes. Free Radic Biol Med 1997;22:1283–8.
9. Meshnick SR, Yang YZ, Lima V, Huypers F, Kamchonwongpaisan S, Yuthavong Y. Iron-dependent free radical generation from the antimalarial agent artemisinin (qinghaosu). Antimicrob Agents Chemother 1993;37:1108–14.
10. Asawamahasakda W, Ittarat I, Pu YM, Ziffer H, Meshnick SR. Reaction of antimalarial endoperoxides with specific parasite proteins. Antimicrob Agents Chemother 1994;38:1854–8.
11. Eckstein-Ludwig U, Webb RJ, Van Goethem ID, et al. Artemisinins target the SERCA of *Plasmodium falciparum*. Nature 2003;424:957–61.
12. Efferth T, Briehl MM, Tome ME. Role of antioxidant genes for the activity of artesunate against tumor cells. Int J Oncol 2003;23:1231–5.
13. Efferth T, Benakis A, Romero MR, et al. Enhancement of cytotoxicity of artemisinins toward cancer cells by ferrous iron. Free Radic Biol Med 2004;27:998–1009.
14. Yang YZ, Little B, Meshnick SR. Alkylation proteins by artemisinin. Effect of heme, pH, and drug structure. Biochem Pharmacol 1994;48:569–73.
15. Dunkern TR, Kaina B. Cell proliferation and DNA breaks are involved in ultraviolet light-induced apoptosis in nucleotide excision repair-deficient Chinese hamster cells. Mol Biol Cell 2002;13:348–61.
16. Sobol RW, Prasad R, Evenski A, et al. The lyase activity of the DNA repair protein β-polymerase protects from DNA-damage-induced cytotoxicity. Nature 2000;405:807–10.
17. Briegert M, Kaina B. Human monocytes, but not dendritic cells derived from them, are defective in base excision repair and hypersensitive to methylating agents. Cancer Res 2007;67:26–31.
18. Kraakman-van der Zwet M, Overkamp WJ, van Lange RE, et al. Brca2 (XRCC11) deficiency results in radioresistant DNA synthesis and a higher frequency of spontaneous deletions. Mol Cell Biol 2002;22:669–79.
19. Adjuik M, Babiker A, Garner P, Olliaro P, Taylor W, White N; International Artemisinin Study Group. Artesunate combinations for treatment of malaria: meta-analysis. Lancet 2004;363:9–17.
20. Gordi T, Lepist EI. Artemisinin derivatives: toxic for laboratory animals, safe for humans? Toxicol Lett 2004;147:99–107.
21. Schmuck G, Roehrdanz E, Haynes RK, Kahl R. Neurotoxic mode of action of artemisinin. Antimicrob Agents Chemother 2002;46:821–7.
22. Efferth T, Volm M. Glutathione-related enzymes contribute to resistance of tumor cells and low toxicity in normal organs to artesunate. In Vivo 2005;19:225–32.
23. Smith SL, Sadler CJ, Dodd CC, et al. The role of glutathione in the neurotoxicity of artemisinin derivatives *in vitro*. Biochem Pharmacol 2001;61:409–16.

Artesunate Derived from Traditional Chinese Medicine Induces DNA Damage and Repair

Paul C.H. Li, Elena Lam, Wynand P. Roos, et al.

Cancer Res 2008;68:4347-4351.